Harmonic Mitigation in an Islanded Microgrid using a DSTATCOM

Megha Goyal, *Student Member, IEEE,* Blessy John and Arindam Ghosh, *Fellow, IEEE*

Abstract **– The degree of proliferation of Distributed Energy Resources (DERs) and application of power electronics appliances are in demand. A microgrid can contain variety of sources such as diesel generator, wind turbine, PV arrays, microturbine and fuel cell. Usually these sources share power where the system frequency changes depending on the power supplied. On the other hand, the microgrid can contain harmonic loads that can affect the performance of the synchronous generators. These deleterious effects of distorting loads can be corrected using a distribution static compensator (DSTATCOM). In this paper, an isochronous control based droop strategy is employed that forces the microgrid to operate at the base frequency of 50 Hz. Therefore the DSTATCOM can be operated at 50 Hz. A closed-loop space vector pulse width modulation (SVPWM) technique is used for the DSTATCOM control. The scheme is validated through the extensive PSCAD/EMTDC simulation studies.**

Index Terms **– Diesel generator, distributed energy resources, DSTATCOM, SPVPM, frequency droop and isochronisation**.

I. Introduction

In the currently changing power supply systems, distributed energy resources (DER) are emerging as a mode to supply efficient and reliable power to customers [1]. The increasing number of renewable energy sources such as photovoltaic, wind and micro-hydro are leading to a substantial amount of electric energy generation in the form of DERs within electric networks. Integration of the DERs will reduce network expansion costs, minimize power losses in long feeders and increase the reliability of networks [2].

DER includes both distributed generators (DGs) and the distributed storage (DS) units [3]. DERs can come of various sizes and types of such as fuel cells, photovoltaic arrays, wind turbines, flywheel and super capacitor etc. A cluster of DGs and load can be considered as a microgrid. It can be operated in a grid connected or in an islanded mode. To control the voltage and frequency of the microgrid in the islanded mode, droop control methods are being used to share the power according to available resources rating. The various kind of droop control strategies are introduced in the literature [4-7]. The traditional method is frequency droop control, in which a microgrid frequency varies within the limit of a frequency band for power sharing based on DG ratings. On the other hand, when only converter interfaced DGs (i.e., DERs) are used, a more responsive angle droop control can be employed. In this, the voltage magnitude and angle of DGs are controlled at a fixed frequency for real and reactive power sharing. An autonomous load sharing technique for parallel connected voltage source converter (VSC) is discussed in [8], in which the improved power-frequency droop scheme is proposed to compute the angle for VSCs directly to yield real power sharing without sacrificing frequency regulation. However, this technique is valid only for VSC interfaced DGs.

A microgrid, which consists group of parallel inverters with linear and non-linear load, several techniques for power sharing with non-linear loads have been discussed in [9-10]. These techniques enable the equal sharing of linear and non-linear loads. If a microgrid consists of inertial generators (e.g. diesel generators) that supply non-linear loads, harmonic current will flow through the armatures of the generators [11]. This will distort the armature reaction, leading to voltage distortion affecting output power. It will also lead to electromagnetic torque pulsation, generating heat and reducing the life of the generators [12, 13]. Therefore, to improve the power quality, capacity, reliability and redundancy, various custom power devices are being used [14]. A DSTATCOM can be used to eliminate load harmonics, as well as, for voltage regulation [15]. Pulse width modulation (PWM) technique is the most popular form for VSC control due its simplicity [16]. On the other hand, space vector pulse width modulation (SVPWM) technique is more efficient for VSC control due to reduced harmonic injection, low switching frequency and losses [17].

In this paper, a new control strategy is proposed for power sharing in the hybrid microgrid, which consists of DGEN and DER with linear and non-linear loads. The microgrid operates in frequency droop control in which frequency deviates within a band depending load and available power. A DSTACOM is connected at the load terminal to eliminate the effect of load harmonics. A closed-loop SVPWM technique is proposed to control the DSTATCOM. The DSTATCOM operates at a constant frequency of 50 Hz. Therefore, the microgrid frequency also needs to be maintained at 50 Hz, irrespective of power drawn by the load. To facilitate this, an isochronous controller is introduced with the frequency droop. It has been shown that the microgrid strictly operates at 50 Hz with the introduction of the isochronous controller.

The rest of the paper is organized as follows. The system structure is presented in Section II, where both frequency droop and isochronous controller are discussed. The DSTATCOM structure and its closed-loop SVPWM control are discussed in Section III. The proposed method is validated through extensive computer simulation studies using PSCAD. The results are discussed in Section IV. The paper concluded in Section V. The system data used are given in Appendix.

The authors thank the Australian Research Council (ARC) for the financial support for this project through the ARC Discovery Grant DP110104554.

The authors are with Department of Electrical and Computer Engineering, Curtin University, Perth, Australia.
Email: megha.goyal@postgrad.curtin.edu.au

II. System Structure

The system structure is shown in Fig. 1. The microgrid contains a diesel generator (DGEN) and a converter interfaced distributed energy resource (DER) that operate in ω-P and Q-V droop control, given by

$$\omega = \omega_r + m \times \left(0.5P^* - P\right) \tag{1}$$

$$V = V_r + n \times (Q^* - Q) \tag{2}$$

where ω_r and ω are the rated and instantaneous frequency of the system respectively in rad/s. The rated and actual real power are denoted by P^* and P respectively. Q^* and Q are the rated and actual reactive power respectively; m, n are the droop coefficients of the frequency and voltage droop lines. The DGEN structure is discussed in [18]. The DER is a dc voltage source that is connected through a three-leg VSC.

Note that in the ω–P droop equation, half the rated power has been used to restrict the frequency variation to within $\pm f_d$ Hz. The droop gain m is chosen accordingly. In this paper, f_d is chosen as 0.5 Hz. Also the rated capacity of the DGEN is 500 kW. Then from (1), we get

$$m_1 = \frac{-f_d \times 2\pi}{(250 - 500)} \text{ rad/kW} \tag{3}$$

In a similar way, the droop gain for the DER can also be calculated.

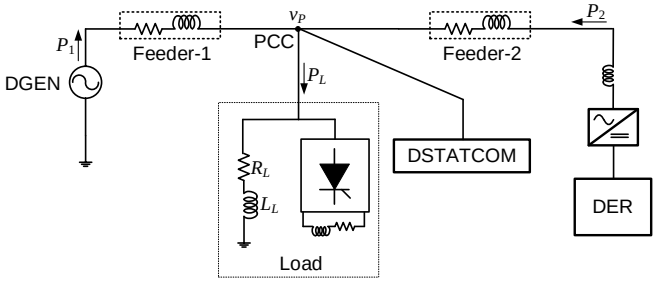

Fig. 1. The microgrid structure under consideration.

A. Isochronous Control

Note that in the frequency droop, given in (1), half the rated power is used such that the frequency can vary ± 0.5 Hz from the fundamental frequency of 50 Hz. The droop coefficients are chosen accordingly to restrict the frequency variation to within these specified limits. However, the DSTATCOM is restricted to operate at the fixed frequency of 50 Hz. Therefore, it is required to recover the droop frequency through an isochronous controller such that both the DGEN and DER operate at 50 Hz.

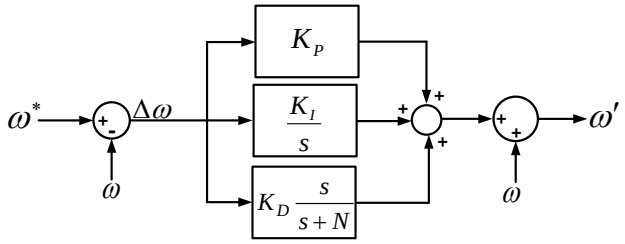

Fig. 2. Schematic diagram of the isochronous controller.

The schematic diagram of the isochronous controller is shown in Fig. 2, which is essentially a PID controller. The frequency obtained from the droop control for each DG, is first compared with the reference (synchronous frequency). The error is then passed through a PID controller. The controller output is added with the droop frequency to obtain ω'. This frequency is then used to control both the DGs.

III. DSTATCOM Structure and Control

The schematic diagram of the DSTATCOM is shown in Fig. 3. In this figure, each switch represents an IGBT and an anti-parallel diode combination. Each phase output contains the LC (L_f-C_f) filter. The resistance R_f represents the converter losses.

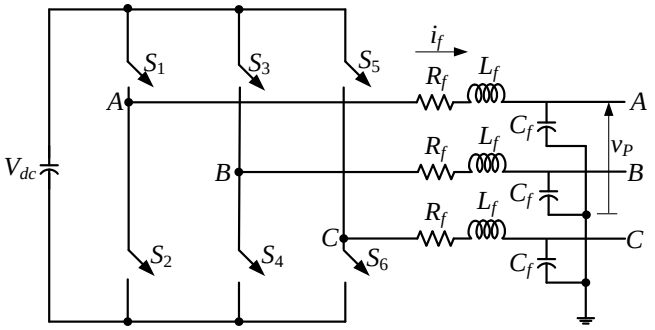

Fig. 3. The DSTATCOM structure.

A. Reference Generation

The main aim is to regulate the voltage PCC voltage against any variation in the load. The load can be non-linear. Let the desired three-phase PCC voltage be given by

$$\begin{aligned} v_{Pa}^* &= |V_P| \sin(\omega t + \delta) \\ v_{Pb}^* &= |V_P| \sin(\omega t + \delta - 120^\circ) \\ v_{Pc}^* &= |V_P| \sin(\omega t + \delta + 120^\circ) \end{aligned} \tag{4}$$

where $|V_P|$ is a pre-specified voltage magnitude, δ is an angle that maintains the power flow from the source to the load and ω is the rated frequency (100π) in rad/s. The angle δ should be such that the required amount of power flows to the load. Also the DSTATCOM needs some amount of power from the microgrid to compensate its switching and internal losses. Note that it is supplied through a dc capacitor. Therefore if the capacitor voltage can be held constant, the required amount of power can flow to the PCC. Based on this logic, a PI controller is designed to regulate the dc voltage and its output sets then angle, given by

$$\delta = K_P \left(V_{dc}^* - V_{dc}\right) + K_I \int \left(V_{dc}^* - V_{dc}\right) dt \tag{5}$$

The DSTATCOM has to synthesize these three-phase voltages at its output.

B. Closed-Loop SVPWM Control

Usually in a PWM control, the voltage at the output of the converter is synthesized in the open-loop and then an LC filter is used to remove the switching harmonics. This may however

cause a phase shift in the output voltage. Therefore a state feedback controller is designed taking into account the filter characteristics and then the switching signals are generated using SVPWM.

Each phase of the DSTATCOM is controlled individually. The first step in the process is to generate instantaneous reference voltages (v_a^*, v_b^* and v_c^*) for the three phases. How these voltages are obtained will be discussed later. The DSTATCOM switches are controlled such that these voltages appear across the filter capacitor (C_f) (or PCC) of the respective phases. However for feedback stabilization, both the voltage across the capacitor and the current through the inductor (i_f) must be controlled. It is to be noted that the current i_f should only contain low frequency components – its high frequency components should be zero. Therefore, we pass this current through a high-pass filter (HPF) and equate it to zero. The feedback control scheme for phase-a is shown in Fig. 4, where the gains k_1 and k_2 are computed using a discrete-time linear quadratic regulator (DLQR). The control output is sampled to form u_a. Similar control law is applied to obtain u_b and u_c for the other two phases [14].

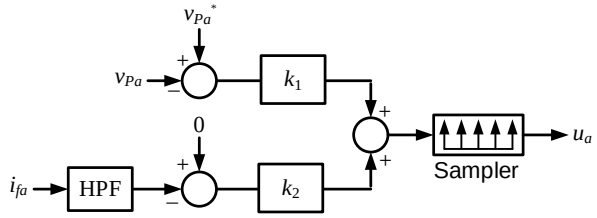

Fig. 4. VSC control output computation.

The three control output values are now used in Clark transformation to a stationery axis as

$$\begin{bmatrix} v_\alpha \\ v_\beta \end{bmatrix} = \frac{2}{3}\begin{bmatrix} 1 & -\frac{1}{2} & -\frac{1}{2} \\ 0 & \frac{\sqrt{3}}{2} & -\frac{\sqrt{3}}{2} \end{bmatrix}\begin{bmatrix} u_a \\ u_b \\ u_c \end{bmatrix} \tag{5}$$

From these, a vector $V\angle\theta$ is computed as

$$V = \sqrt{v_\alpha^2 + v_\beta^2}$$
$$\theta = \tan^{-1}\left(\frac{v_\alpha}{v_\beta}\right), \quad \theta \in [0, 360^\circ] \tag{6}$$

The space vector is divided into 6 sectors, where Sector 1 is in between $0° < \theta < 60°$ and so on, as shown in Fig. 5 (a). Each triangular sector is formed by two active state vectors of amplitude (2/3) V_{dc}. After determining the sector, the reference space vector V can be mapped into two adjacent vectors as shown in Fig. 5 (b), where T_a and T_b respectively denote the time duration for active vector V_1 and V_3.

The vector V can then be defined in terms of switching instants as

$$V = \frac{T_a}{T_s}\times V_1 + \frac{T_b}{T_s}\times V_3 + \frac{T_0}{T_s}\times V_0 \tag{7}$$
$$T_0 = T_s - (T_a + T_b) \tag{8}$$

where T_s is the half of the switching frequency and T_0 is the time period for the zero-vector. These times are calculated as given in [19]. The zero vectors V_0 and V_7 are symmetrically distributed in each switching period to reduce the switching losses [20]. The switching time for each sector is as given in Table I [17]. These control signals are compared to a triangular carrier to generate the switching pulses for upper and lower switches of three phases. Moreover, the DC link voltage is efficiently utilized in SVPWM as compared to sinusoidal PWM.

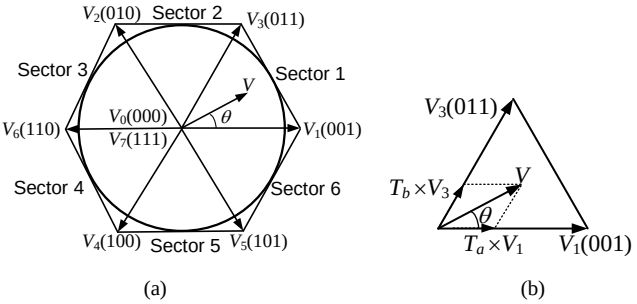

Fig. 5. (a) Sector definition and (b) active vector states.

TABLE I: SWITCHING TIME FOR EACH SECTOR.

Sector	Upper switches	Lower Switches
1	$S_1 = T_a + T_b + T_0/2$ $S_3 = T_b + T_0/2$ $S_5 = T_0/2$	$S_2 = T_0/2$ $S_4 = T_a + T_0/2$ $S_6 = T_a + T_b + T_0/2$
2	$S_1 = T_a + T_0/2$ $S_3 = T_a + T_b + T_0/2$ $S_5 = T_0/2$	$S_2 = T_b + T_0/2$ $S_4 = T_0/2$ $S_6 = T_a + T_b + T_0/2$
3	$S_1 = T_0/2$ $S_3 = T_a + T_b + T_0/2$ $S_5 = T_b + T_0/2$	$S_2 = T_a + T_b + T_0/2$ $S_4 = T_0/2$ $S_6 = T_a + T_0/2$
4	$S_1 = T_0/2$ $S_3 = T_a + T_0/2$ $S_5 = T_a + T_b + T_0/2$	$S_2 = T_a + T_b + T_0/2$ $S_4 = T_b + T_0/2$ $S_6 = T_0/2$
5	$S_1 = T_b + T_0/2$ $S_3 = T_0/2$ $S_5 = T_a + T_b + T_0/2$	$S_2 = T_a + T_0/2$ $S_4 = T_a + T_b + T_0/2$ $S_6 = T_0/2$
6	$S_1 = T_a + T_b + T_0/2$ $S_3 = T_0/2$ $S_5 = T_a + T_0/2$	$S_2 = T_0/2$ $S_4 = T_a + T_b + T_0/2$ $S_6 = T_b + T_0/2$

IV. Simulation Results

In this section, simulation studies are performed using PSCAD. Three different case studies are presented. The microgrid data are given in Table I and the DSTATCOM data are given in Table II in Appendix.

A. Case-1: Isochronous Operation

In this example, only the RL load is assumed to be present. Also the DSTATCOM is not connected. The system response from a cold start is shown in Fig. 6. The load power and the power supplied by the DGs are shown in Fig. 6 (a). The total load demand (P_L) is 205 kW, the DGEN supplies (P_1) 147 kW and the DER supplies (P_2) 58.8 kW. Therefore the ratio of P_1 is to P_2 is 2.5:1, which is exactly the ratio of the rated power of these two DGs. Since P_1 = 147 kW, from (3) the system frequency without the isochronous controller will be 50.206 Hz. However, with the isochronous controller, the frequencies of both DGs become 50 Hz within 2.5 s, as shown in Fig. 6 (b).

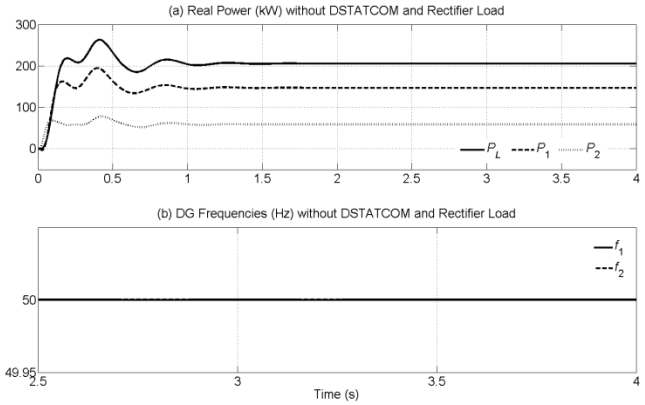

Fig. 6. Microgrid system behavior when the DSTATCOM and the rectifier load are not connected.

B. Case-2: MG Operation with DSTATCOM and Rectifier Load

In this example, both the rectifier load and the DSTATCOM are connected at the beginning (cold start). The total load demand is 500 kW. The flow of active power through the system is shown in Fig. 7 (a). It can be seen that power sharing ratio is 2.5:1, while the DSTATCOM absorbs negligible power. The frequency settles at 50 Hz due to isochronous control. It is to be noted that the load power will contain distortion due to the presence of harmonics. However only the average power is shown here and hence the distortions are not visible.

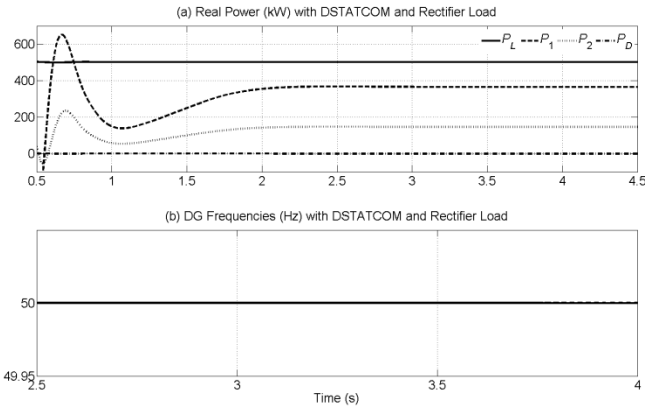

Fig. 7. Power flow and frequency in the microgrid when the DSTATCOM and the rectifier load are connected.

The dc capacitor voltage is shown in Fig. 8 (a). It can be seen that it settles to the desired voltage of 16 kV within 2 s. The output of angle controller is shown in Fig. 8 (b). The steady state tracking performance of the DSTATCOM is shown in Fig. 8 (c), where the desired voltage and the tracking error are plotted. The tracking error is insignificant compared to the desired voltage, which indicates a satisfactory voltage tracking performance with the closed-loop SVPWM control The instantaneous currents of phase-a are shown in Fig. 9. It can be seen that the load current is distorted, while the currents supplied by the DGEN and DER are sinusoidal due the voltage correction by the DSTATCOM. Note that the switching frequency for the SVPWM control is 2.5 kHz. For a comparable performance from a PWM control can be achieved with a switching frequency of 15 kHz.

C. Case-2: MG Operation during a Load Change

With the system operating in the steady state, the linear RL load is suddenly increased by 100 kW at 5 s. From the plots given in Fig. 10 (a), it can be seen that both the DGs increase their power output in the specified ratio, while the power from/to the DSTATCOM remains unchanged. The DG frequencies come back to their steady state values within 0.5 s. The angle controller is effective as dc capacitor voltage and the angle settle within 2 s.

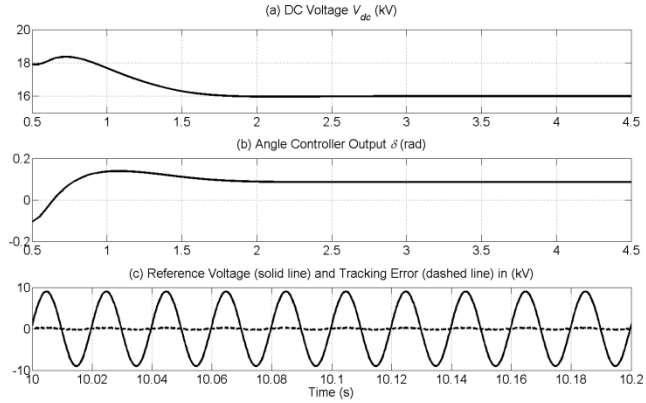

Fig. 8. DC capacitor voltage, angle and DSTATCOM tracking performance.

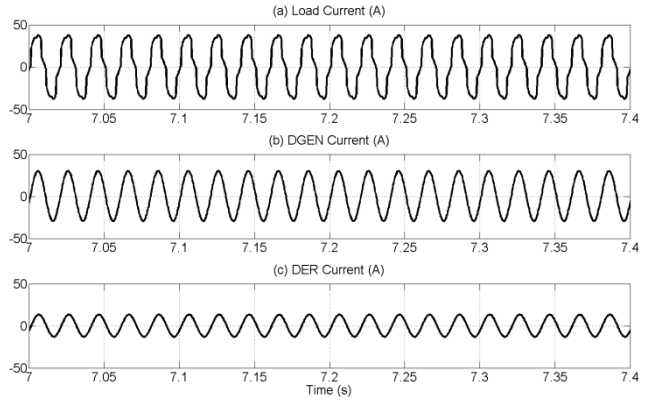

Fig. 9. Phase-a load, DGEN and DER currents.

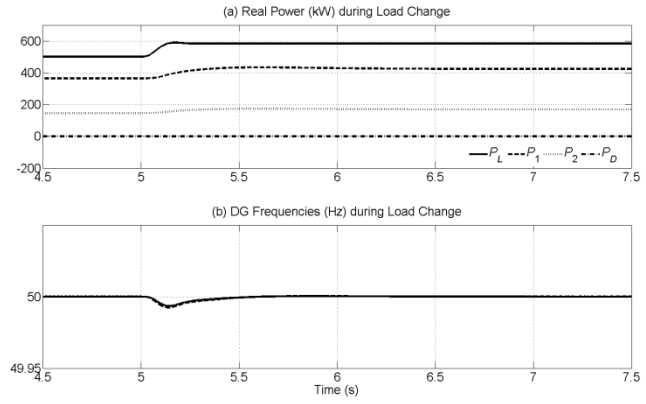

Fig. 10. Power flow and frequency in the microgrid during load change.

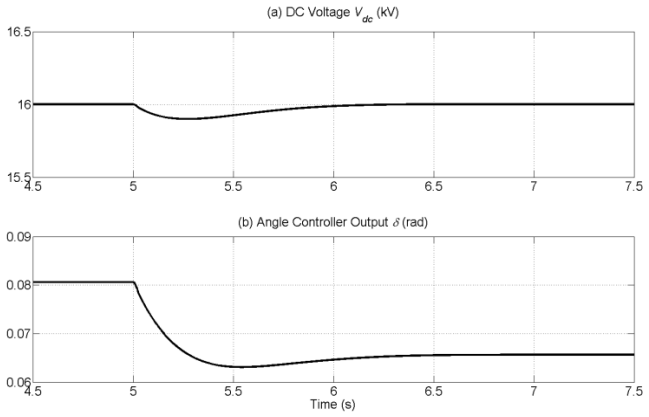

Fig. 11. DC capacitor voltage and angle during load change.

V. Conclusions

This paper introduces a new control strategy for a microgrid that contains non-linear loads. Based on this control strategy, the microgrid operates at a set reference frequency while sharing power in a frequency droop control. An isochronous control method is proposed to maintain the microgrid system frequency at 50 Hz. As a consequence, a DSTATCOM that injects voltage at 50 Hz can be used at the load terminal to prevent the harmonic currents drawn by the load harmonics to travel to the diesel generator terminals. The DSTATCOM is controlled through a closed-loop SVPWM control technique base on linear quadratic control. A few case studies are presented to validate the proposed control strategy.

References

[1] F. Katiraei, R. Iravani, N. Hatziargyriou, and A. Dimeas, "Microgrids Management," *Power and Energy Magazine, IEEE* , vol.6, no.3, pp.54-65, May–June 2008.

[2] J. M. Guerrero, F. Blaabjerg, T. Zhelev et al, "Distributed generation: toward a new energy paradigm," *IEEE Industrial Electronics Magazine*, pp. 52-64, March 2010.

[3] B. Kroposki, R. Lasseter, T. Ise, S. Morozumi, S. Papatlianassiou, and N. Hatziargyriou, "Making microgrids work," *Power and Energy Magazine, IEEE* , vol.6, no.3, pp. 40-53, May-June 2008.

[4] J. C. Vasquez, J. M. Guerrero, A. Luna, P. Rodríguez, and R. Teodorescu, "Adaptive droop control applied to voltage-source inverters operating in grid-connected and islanded modes," *IEEE Trans. Ind. Electron*., vol. 56, no. 10, pp. 4088-4096, Oct. 2009.

[5] J. He; Y. W. Li, "An Enhanced Microgrid Load Demand Sharing Strategy," *IEEE Transactions on Power Electronics*, vol.27, no.9, pp. 3984-3995, Sept. 2012.

[6] C-.T. Lee, C. C. Chu, and P. T. Cheng, "A New Droop Control Method for the Autonomous Operation of Distributed Energy Resource Interface Converters," *IEEE Transactions on Power Electronics*, vol.28, no.4, pp.1980-1993, April 2013.

[7] R. Majumder, A. Ghosh, G. Ledwich, and F. Zare, "Power Management and Power Flow Control with Back-to-Back Converters in a Utility Connected Microgrid," *IEEE Transactions on Power System*, vol. 25, no. 2, pp. 821-834, May 2010.

[8] C. K. Sao, and P. W. Lehn, "Autonomous load sharing of voltage source converters," *IEEE Transactions on Power Delivery*, vol.20, no.2, pp.1009-1016, April 2005.

[9] A. Tuladhar, H. Jin, T. Unger, and K. Mauch, "Control of parallel inverters in distributed AC power systems with consideration of line impedance effect," *IEEE Transactions on Industry Applications*, vol.36, no.1, pp.131-138, Jan/Feb 2000.

[10] U. Borup, F. Blaabjerg, and P. N. Enjeti, "Sharing of nonlinear load in parallel-connected three-phase converters," *IEEE Transactions on Industry Applications*, vol.37, no.6, pp.1817-1823, Nov/Dec 2001.

[11] A. H. Samra, and K. M. Islam, "Harmonic effects on synchronous generators voltage regulation," *IEEE Southeastcon '95. Visualize the Future*, pp.376-380, Mar 1995.

[12] W. Jin-quan, S. Peng-chao, C. Chen-hua, L. Jian-ke, and Y. Tao, "Analysis of Operation of Synchronous Generator under the Distortion of Harmonic Current," *Asia-Pacific Power and Energy Engineering Conference (APPEEC)*, pp.1-4, March 2012.

[13] M. W. Davis, R Broadwater, and J. Hambric, "Modeling and Testing of Unbalanced Loading and Voltage Regulation," NREL report number NREL/SR-581-41805, July, 2007.

[14] A. Ghosh, and G. Ledwich, "Stability of hysteretic controlled voltage source converters in a power system," *IEEE PES Innovative Smart Grid Technologies Asia (ISGT)*, pp.1-8, Nov. 2011.

[15] A. Ghosh and G. Ledwich, "Load compensating DSTATCOM in weak AC Systems," *IEEE Trans. on Power Delivery*, vol. 18, pp. 1302-1309, Oct. 2003.

[16] H.W. van der Broeck, H.-C. Skudelny, and G. V. Stanke, "Analysis and realization of a pulse width modulator based on voltage space vectors," *IEEE Transactions on Industry Applications*, vol.24, no.1, pp.142-150, Jan/Feb 1988.

[17] D. Sasi, and P. J. Kuruvilla, "Modelling and simulation of SVPWM inverter fed permanent magnet brushless dc motor drive," *International Journal of Advanced research in Electrical, Electronics and Instrumentation Engineering*, Vol. 2, No. 5, May 2013.

[18] M. Goyal, and A. Ghosh, "A Phase–Locked–Loop Design for the Smooth Operation of a Hybrid Microgrid," *Australian Universities Power Engineering Conference* (*AUPEC*), pp. 46-51, Sep. –Oct. 2013.

[19] Y. Ma, L. Fan, and Z. Miao, "Realizing space vector modulation in MATLAB/Simulink and PSCAD," *North American Power Symposium (NAPS)*, pp.1-6, Sept. 2013.

[20] V.H. Prasad, D. Boroyevich and R. Zhang, "Analysis and comparison of space vector modulation schemes for three-leg and four leg voltage source inverters," *IEEE Applied Power Electronics Conference and Exposition*, Vol. 2, pp. 864-871, February 1997.

Appendix

Table I. Parameters of the DGs connected to the Microgrid

System Quantities	**Values**
Feeder impedance	R_{f1} = 1.21 Ω, L_{f1} = 38.5 mH R_{f2} = 2.42 Ω, L_{f2} = 77.0 mH
DGEN Rating	500 kW
DER Rating	200 kW
Load-1	R_{La}=272 Ω, L_{La} = 419 mH R_{Lb}=272 Ω, L_{Lb} = 419 mH R_{Lc}=272 Ω, L_{Lc} = 419 mH
Non-Linear Load	Full bridge rectifier with a load of 1000 Ω and 100 mH.
Droop Coefficient (Frequency–Voltage)	
m_1	0.0126 rad/MWs
m_2	0.0314 rad/kWs
n_1	0.02 kV/MVAr
n_2	0.05 kV/MVAr

Table II. Parameters of DSTATCOM

Parameters	**Values**
R_f	0.001 Ω
C_f	50 μF
L_1	33 mH
V_{dc}	13.5 kV
PI controller parameters	
Proportional gain	-0.1
Integral gain	-0.25

Table III. Parameters of Isochronous (PID) Controller

System data	**Value**
Proportional gain (K_P)	0.1
Integral gain (K_I)	10
Differentiator gain (K_D)	0.004
Constant coefficient (N)	200